The Generation of Runoff From Subarctic Snowpacks

THOMAS DUNNE

Department of Geological Sciences, University of Washington, Seattle, Washington 98195

ANTHONY G. PRICE

Department of Geography, University of Toronto, Scarborough, Ontario, Canada

SAMUEL C. COLBECK

U.S. Army Cold Regions Research and Engineering Laboratory, Hanover, New Hampshire 03755

A physically based model of the movement of water through snowpacks was used to calculate hydrographs generated by diurnal waves of snowmelt on the tundra and in the boreal forest of subarctic Labrador. The model was tested against measured hydrographs from hillside plots that sampled a range of aspect, gradient and length, vegetative cover, and snow depth and density. The model yielded good results, particularly in the prediction of peak runoff rates, though there was a slight overestimate of the lag time. A comparison of predictions with field measurements indicated that given the ranges over which each of the controls is likely to vary, the two most critical factors controlling the hydrograph are the snow depth and the melt rate, which must be predicted precisely for short time intervals. Permeability of the snowpack is another important control, but it can be estimated closely from published values.

INTRODUCTION

In a previous paper [*Price and Dunne*, 1976], we dealt with the calculation of hourly snowmelt on hillsides with varying aspect, gradient, and vegetative cover by using an hourly energy budget. The work demonstrated significant differences between daily totals of melt and between the timing of melt in the various environments (see *Price* [1975] for further examples). In this paper we consider the computation of runoff generated by snowmelt on the hillside plots on the tundra and under the boreal forest of subarctic Labrador.

PREVIOUS WORK ON SNOWMELT RUNOFF

Gerdel [1945] measured the rate of movement of water through ripe snowpacks. He showed that the water-holding and transmission characteristics of ripe snow are much like those of coarse sand. After melting at the surface has ceased, water drains rapidly from the snowpack, which soon attains an irreducible water content in the range 1–10% by volume. *Anderson* [1968] employed an empirical technique for routing water through the snowpack by comparing graphs of computed hourly snowmelt with hydrographs of runoff measured in a lysimeter beneath the snow. *Dunne and Black* [1971] presented a qualitative discussion of snowmelt runoff hydrographs generated by flow along surface, shallow subsurface, and deeper subsurface paths on three hillside plots in Vermont.

Colbeck [1971, 1972] developed a physical model of the percolation of meltwater through a ripe snowpack. The model first considers the unsaturated flow path from the melting surface to the base of the pack. Calculated hydrographs at various depths in the unsaturated zone were tested against field measurements by *Colbeck and Davidson* [1973] in a very deep snowpack in the Cascade Mountains of Washington. Some uncertainties were produced by the presence of ice lenses in the pack, but the results were generally satisfactory.

Later, *Colbeck* [1974] treated the movement of water after it has percolated to the bottom of the snowpack. If the infiltration capacity of the soil exceeds the rate of percolation of meltwater, all the water will enter the soil and will move to a stream channel as relatively rapid subsurface flow or will recharge the deeper groundwater and supply streamflow later in the year. Since rates of melting are usually low, the infiltration capacities of many soils are not exceeded by snowmelt. Where the infiltration capacity is lowered by the presence of concrete frost or saturation, the percolating meltwater accumulates and forms a thin saturated layer at the base of the snowpack and moves downslope through the snow [*Dunne and Black*, 1971]. *Colbeck*'s [1974] model describing this downslope flow in a thin saturated layer had not been tested against field measurements. In this paper we report an application of the combined models of unsaturated and saturated flow to the calculated snowmelt reported in our previous paper. The result of these calculations is a runoff hydrograph from the base of a hillslope. We have checked our calculations against measured hydrographs of overland flow from hillside plots ranging in size from 1335 to 2810 m^2. Our results confirm the value of the runoff model and point to the parameters which should be estimated with care for successful application of the procedure.

THE RUNOFF MODEL

For the derivation of the runoff model the reader is referred to the previously mentioned papers by Colbeck. Only the summary equations to be applied to the field situation are given here.

Percolation of water through the snowpack is treated in two steps (see Figure 1). Melting at the surface releases a diurnal wave of water which travels vertically through the unsaturated snowpack. As it accumulates at the base of the pack, the water travels in a thin saturated zone to the base of the slope.

The Unsaturated Zone

In considering the meltwater released at a flux rate m at any time, ignoring capillary effects which are minor, *Colbeck* [1971] shows that the vertical rate of movement of this value of flux is given by

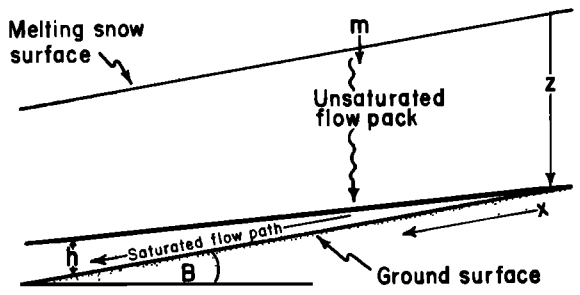

Fig. 1. The path of water flow through the snowpack.

$$\left(\frac{dz}{dt}\right)_m = \frac{n}{\phi_e}\left(\frac{\rho g k_u}{\mu}\right)^{(1/n)} m^{[(n-1)/n]} \qquad (1a)$$

where n is an exponent in the relationship

$$k(S) = k_u S^n \qquad (1b)$$

where S is the degree of saturation of the snowpack; $k(S)$ is the permeability of snow in the unsaturated zone to water at some fixed value of S, and k_u is the intrinsic permeability of the snow in the unsaturated zone, and

$$\phi_e = \phi(1 - S_i) \qquad (1c)$$

where

ϕ_e effective porosity of the snowpack;
S_i irreducible saturation of the snowpack;
ϕ total porosity of the snowpack;
ρ density of water;
g acceleration due to gravity;
m melt rate (i.e., the flux rate of water originating at the surface of the snowpack).

If we consider a flux of meltwater being generated at the snow surface at a flux rate m and if we know the depth of the snowpack z on that day, (1a) allows us to calculate the time of arrival of that value of flux at the base of the snowpack. The hydrograph generated by doing this for successive time periods is the input to the saturated layer. We will demonstrate the technique with an example later in the paper. Since this input can vary in space and time, we will refer to it as $I(x, t)$.

The Saturated Layer

For a strip of hillside of unit width with constant small angle β, *Colbeck* [1974] expresses the continuity equation for the saturated layer as

$$\frac{k_s \rho g \beta}{\mu} \cdot \frac{\partial h}{\partial x} + \phi \frac{\partial h}{\partial t} = I(x, t) \qquad (2)$$

where

k_s intrinsic permeability of the saturated layer;
h thickness of the saturated layer (see Figure 1);
x distance along the hillslope;
t time.

This equation indicates that the thickness of the saturated layer varies with distance downslope and with time in response to the input of water percolating from the unsaturated zone. In the case of daily cycles of snowmelt from a pack of uniform thickness the input is constant along the slope at any one time but varies throughout the day in the form of a wave in response to variations in the energy available for melting. These waves of melt generate daily waves of vertical flow through the unsaturated zone, and in the saturated zone a wave travels downslope each day.

Let us assume that an observer moves downslope with the wave in the saturated zone and let his position in time and space be fixed by coordinates x' and t' moving at the wave speed C_s, such that $x' = x - C_s t$, $t' = t$, where the wave speed in the saturated layer is given by

$$C_s = (\rho g/\mu)(k_s \beta/\phi) \qquad (3)$$

In this new coordinate system, (2) reduces to

$$\partial h/\partial t' = [I(x, t)]/\phi \qquad (4)$$

which when integrated and multiplied by the flux rate yields

$$q(0, t_L') = \frac{\rho g k_s \beta}{\phi \mu} \int_{t_0'}^{t_L'} I(0, t')\, dt' \qquad (5)$$

where t_0' and t_L' are time limits for the period during which a small parcel of water entering the saturated layer at the top of the hillside moves to the base of the slope. Equation (5) states that the discharge from the base of the hillslope $q(0, t_L')$ is equivalent to the input to the saturated layer from the unsaturated zone integrated over a preceding period equal to the time taken for the water to move through the saturated layer $(t_L' - t_0') = L_s/C_s$, where L_s is the length of the hillslope.

Equation (5) is in units of cubic centimeters per hour per centimeter of width of the hillside, and to be converted to units of centimeters per hour, in which we calculated the original snowmelt input rates, it must be divided by the area of the unit strip of hillside L_s. Equation (5) therefore becomes

$$Q(0', t_L') = \frac{1}{(t_L' - t_0')} \int_{t_0'}^{t_L'} I(0, t')\, dt' \qquad (6)$$

which gives the flux rate (Q) at the hillslope base in centimeters per hour, i.e., the predicted hillslope snowmelt hydrograph.

The Field Study

The Hillside Plots

The runoff model was applied to the prediction of snowmelt hydrographs from hillside plots under boreal forest and on the tundra of the Labrador subarctic, near Schefferville, Quebec (elevation of 540 m, latitude of 54°52'N, and longitude of 67°01'W). The physical geography of the region and of the plots has been described previously [*Price and Dunne*, 1976]. Only the details relevant to the prediction of runoff are included here.

The cover and geometry of the seven plots are summarized in Table 1. Although the hillslopes are not exactly straight, considerable proportions of them are, and we considered the approximation of constant β to be justified.

The soils of the plots are minipodzols, developed in a dense silty glacial till. Even during summer these soils have a low permeability. During the autumn, however, they are invaded by concrete frost [*Post and Dreibelbis*, 1942] and rendered impermeable. During the melt season we dug pits to examine the soil and found no infiltration beneath the snowpack. On the upper parts of the tundra sites no soil covered the bedrock, but the rock was also rendered impermeable by frost. In fact, the tundra sites were underlain by permafrost. Only during the last few days of the melt did we observe any percolation of meltwater into the soil. The surface of the soil on all the sites was covered by a mat of lichens (mainly caribou moss or *Cladonia alpestris*). When they are saturated and buried by snow, the lichens are compressed and lie very close to the

TABLE 1. Cover and Geometry of the Hillside Plots

Experimental Site	Cover	Area, m²	Length (L_s), m	Angle (β), degrees
A	Tundra	2810	85	4
B	Tundra	1335	49	9
C	Tundra	1777	37	5
D	Forest	2409	85	7
E	Forest	1802	54	15
F	Forest	1822	61	5.5
G	Forest	1680	76	7

surface of the frozen mineral soil. Excavations that we made into the snowpack showed that the saturated layer was almost all within the snow. A small amount of water was percolating through the compressed lichen mat, but this was treated like flow through the snow.

Instrumentation of the Plots

At the base of each plot was a 30.5-m-long runoff collector. Each runoff collector consisted of a surface channel and a 1-m deep trench equipped with a drain tile, as shown in Figure 2. Water from the surface and subsurface systems was piped to weir boxes where a continuous record of stage at the calibrated weirs gave a continuous record of discharge at each site. During the 1972 season, runoff was measured from both the forested and tundra sites until the sites on the tundra were destroyed by flooding. During the 1973 season a continuous record of runoff was obtained only at the forested sites.

Descriptive Hydrology

Each day during the snowmelt period the sun rose at approximately 0430 hours. It irradiated the various plots in a sequence determined by their aspect, but insolation generally reached a peak between 1100 and 1230 hours. The rate of melting usually peaked between 1330 and 1430 hours, since turbulent fluxes of sensible and latent heat increased during the afternoon. Melt continued throughout some nights when the warm sector of a large depression lay over the area and provided large inputs of sensible and latent heat to the snowpack. On other days melt usually began between 0730 and 0930 hours and continued until about 1730–2130 hours.

No subsurface runoff was measured in the trenches during the snowmelt period. The soil was rendered impervious by concrete frost, as described previously. Only after the snow cover had melted completely did a very small amount of flow drain from the tiles in the trenches. Surface runoff occurred each day during the melt and generated the expected strong diurnal wave. Early in the melt period, surface melting stopped during the night, but water continued to drain from the pack throughout the night. Figure 3 shows an example of the surface hydrographs from 1 day of melt on two of the plots and indicates most of the characteristics of runoff that must be explained. Plot E is a steep hillside with a thin snowpack, while D has a gentler gradient and an average snowpack depth almost four times as great as that on E on the day in question. In spite of the difference between their aspects and gradients the differences between the plots in the timing of snowmelt on that day was insignificant by comparison with the differences in the timing of runoff. The shapes of the hydrographs were controlled primarily by the depth of the snowpack and the angles and lengths of the hillslopes. The rates of melting, however, also play a role in controlling the rate of response of the hydrograph, as is indicated in (1*a*).

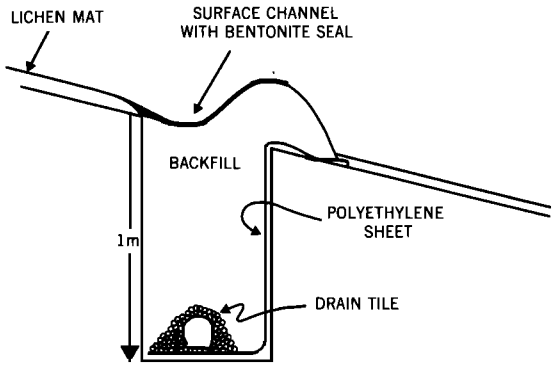

Fig. 2. The runoff collection system.

On May 9, 1973, melt began at approximately 0630 hours, 2 hours after sunrise, reached a peak during the fifteenth hour of the day, and declined throughout the following night. Drainage of water from the snowpack continued to decline until the twelfth hour on both plots. Runoff from E then rose sharply to a peak of 0.36 cm/h at 1500 hours and declined rapidly, while the drainage from D rose more slowly to a peak of 0.30 cm/h at 1930 hours. Differences in the total volume of melt were related to variations in the total radiation received, and to differences of wind speed and of surface roughness [see *Price and Dunne*, 1976]. The hydrographs from plots F and G (see Figure 4) peaked several hours after that from plot D and declined even more slowly.

Figure 4 shows a sequence of daily hydrographs from the forest plot G with a deep snowpack to show the daily differences in form of the hydrographs from one plot. The recession limbs from each day were extrapolated beneath those of succeeding days by fitting a semilogarithmic curve to the declining limb. Calculations using the physical model later showed that this extrapolation was accurate and that the hydrographs from some days should in fact be extrapolated for 60 or more hours after the peak. This separation procedure was used to calculate the volumes of runoff generated each day.

Volumes of runoff ranged from very small values up to 5.9 cm/d. Peak rates of runoff also varied from small values at the

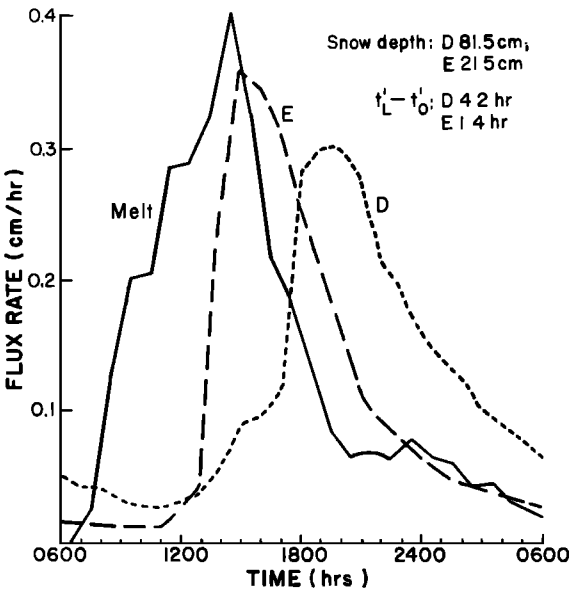

Fig. 3. Hydrographs of surface melting and runoff from plots D and E in the boreal forest on May 9, 1973.

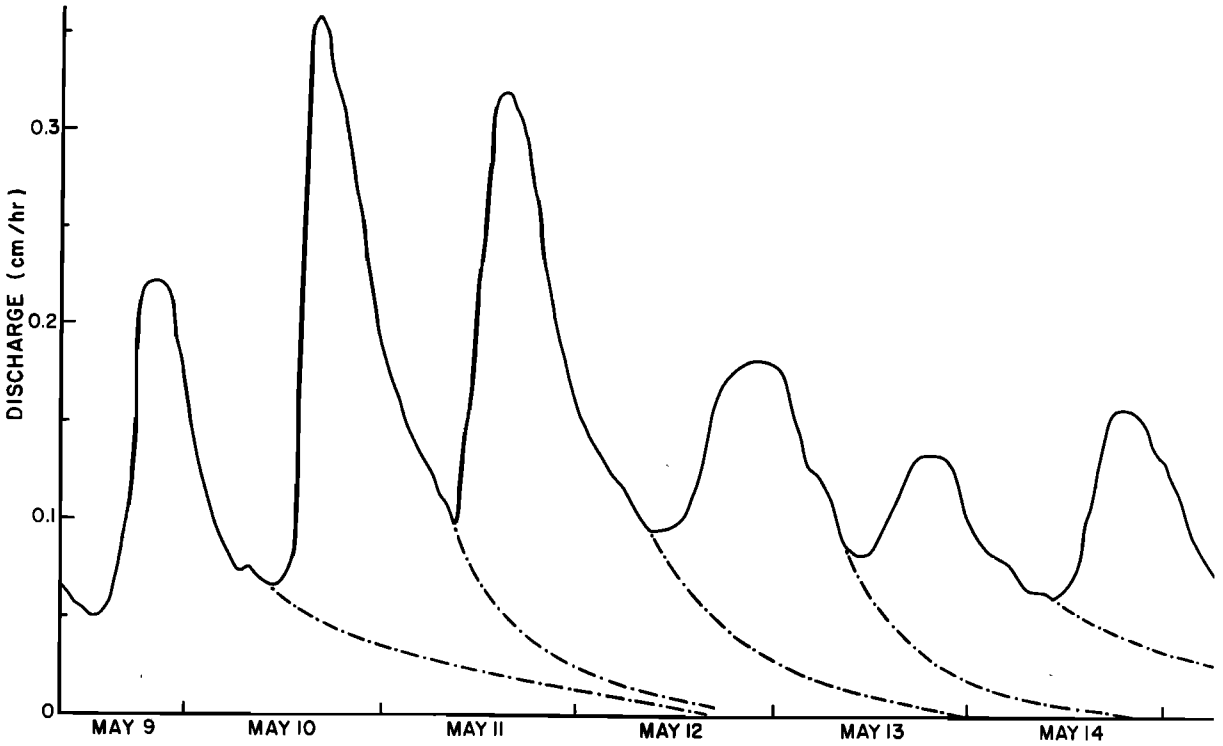

Fig. 4. Hydrographs of surface runoff from plot G in the forest in May 1973.

beginning and end of the melt up to rates between 0.35 and 0.46 cm/h on the various plots. The plots which received the highest rates of insolation or which had the thinnest vegetation cover and greatest wind speeds did not necessarily generate the largest runoff peaks. The pattern was complicated by the fact that the snow cover broke up first on the plots which originally had the thinnest snow packs. By the time meteorological conditions were most conducive to melting, the snow cover on some of the plots had already begun to break up, and so only a portion of these plots could generate runoff. The highest daily melt total (5.9 cm) and the highest peak runoff rate (0.46 cm/h) were both recorded on plot F, the most northerly facing and densely wooded plot, which was still completely covered by snow when, late in the season, very high sensible and latent heat fluxes associated with the warm sector of a large depression caused high rates of melting.

The timing of runoff also showed no simple pattern. There was a general decrease in the time lapse between the onset of melting and the time at which the daily hydrographs began to rise. There was also a general decrease in the lag between the peak of melting and the peak runoff rate. Those changes were associated with a thinning of the snowpack. The relationship between lag time and snow depth, however, was complicated by such factors as the pattern of flux rates generated at the surface, especially the peak flux rate, light falls of snow during the melt season, and the breakup of the snowpack.

The hydrographs from the tundra sites were similar to those from the forest in general form, but the initiation of melting usually occurred later on the tundra as a result of the greater nighttime heat deficits caused by higher wind speeds, lower air temperatures, and possibly greater long-wave radiation losses.

The duration of the melt season varied from 7 days for the shallow snowpack on site C to 27 days for the deepest pack on site F, the plot with the most northerly aspect.

Application of the Runoff Model

To illustrate the procedure for computing runoff from a hillside, we will use data for melt and runoff of 1 day from plot A on the tundra.

The Unsaturated Zone

For a constant flux rate m, (1a) can be integrated to yield

$$z = \frac{n}{\phi_e}\left(\frac{\rho g k_u}{\mu}\right)^{1/n} m^{[(n-1)/n]} t + C \qquad (7)$$

If $t = 0$ is the time at which the flux m leaves the snow surface, $z = 0$ when $t = 0$, and so $C = 0$. Equation (7) describes the depth of penetration of a flux of meltwater with constant flux rate m at any time t. Alternatively, if we set z equal to the depth of the snowpack, we can use the equation to calculate the time of arrival of the flux of meltwater m at the base of the snowpack. For a constant flux rate, permeability, n, and porosity the travel time of the flux is a linear function of depth.

Application of (7) requires an estimate of k_u, the intrinsic permeability of the unsaturated zone of the snowpack, which is chiefly determined by crystal size. It changes rapidly during the ripening of the pack and then only slowly as crystal size increases during the melt. It also changes with depth in the snowpack if significant variations of crystal size and snow or ice density occur; but the uniformity of the Schefferville snowpacks, which had not experienced midwinter melts, suggested that such vertical variation could be ignored for our study. We did not measure k_u directly in the field. Instead, we measured crystal sizes of approximately 2 mm in the unsaturated zone and calculated permeability from *Shimizu*'s [1970] experimental results. The density of the snow at Schefferville being taken into account, the permeability of snow in the unsaturated zone was estimated to be 6×10^{-6} cm^2.

A value must also be estimated for n defined in (1*b*). Field evidence given by *Colbeck and Davidson* [1973] suggests that n is approximately equal to 3 for snow. In the absence of an extended set of laboratory measurements to define (1*b*) for the Schefferville snow, we adopted this value.

To derive the effective porosity ϕ_e we considered a unit volume of the snowpack containing only its irreducible water content. The total mass of ice and water in the unit is numerically equal to the snowpack density, for which we took an average field measurement of 0.42 g/cm³ for the tundra sites. This value is equal to the sum of the masses of ice and water in the unit volume; i.e.,

$$0.42 \text{ g} = S_i\phi\rho + (1 - \phi)\rho_i \qquad (8)$$

where ρ_i is the density of ice (0.92 g/cm³ at 0°C). We chose a value of 0.08 for S_i [*Gerdel*, 1945]. Substitution of the values of ρ, ρ_i, and S_i into (8) gives a value of 0.59 for ϕ, and substituting this value into (1*c*) yields $\phi_e = 0.544$. As the measured density of the snowpack in the forest was less than that on the tundra, the computed value of ϕ_e for the forest was 0.652.

Using these estimated and derived values for the parameters of the snowpack, we can rewrite (7) as

$$z = 59.0 \text{ m}^{2/3} t \qquad (7a)$$

which shows that for chosen flux rates the depth of penetration is a linear function of time.

Now we consider the movement of values of meltwater flux originating at the surface ($z = 0$) at chosen times. Their flux rates m are given by the computed rate of melting at that time [from *Price and Dunne*, 1976], as shown in Figure 5. This value is substituted into (7*a*), and a line representing the penetration of that parcel as a function of time is drawn, as shown in Figure 6. The procedure is repeated for any chosen number of flux rates and times of origin. The slopes of the lines increase on the rising limb of the hydrograph and decline on the recession limb.

Since the rate of penetration of a value of flux is related to the flux rate at which it was generated, larger fluxes overtake smaller ones. Immediately before the increase of melting rate on the morning of May 16 in Figure 5, the declining flux rate was 0.019 cm/h at the surface. During the hour 1030–1130 the melt rate began to increase, and at 1040 had risen to 0.05 cm/h. The penetration of this flux into the snowpack is represented in Figure 6 by the line rising from 1040 at a rate of 8.02 cm/h. This flux, since it is traveling faster than the 0.019 cm/h flux, will overtake the latter at some depth in the pack, creating an instantaneous increase of flux rate at that depth. *Colbeck* [1971] has described this instantaneous increase of flux rate as a 'shock front' which travels down through the snowpack. The front overrides the slower moving fluxes (m_-) and is in turn overriden by larger faster fluxes (m_+). The rate of propagation of the shock front ($d\xi/dt$) depends upon both m_- and m_+ in the following manner [*Colbeck*, 1974]:

$$\frac{d\xi}{dt} = \left(\frac{\rho g k_u}{\mu}\right)^{1/3} \phi_e^{-1}(m_-^{2/3} + m_-^{1/3}m_+^{1/3} + m_+^{2/3}) \qquad (9)$$

At the depth and time at which the 0.019 cm/h flux is overtaken by the 0.05 cm/h flux, therefore, the shock front is traveling downward at 6.0 cm/h. The shock front travels at a rate that is intermediate between the rates of the two fluxes which produce it.

Consider, for example, the circled point in Figure 6, where a flux of 0.40 cm/h overtakes the shock front at the instant at which the front itself is overriding an earlier slower flux of 0.021 cm/h from the melt of the previous day. At that point the speed of the shock front is given by (9), with $m_- = 0.021$ and $m_+ = 0.40$. From this point the shock front moves down at a speed of 16.2 cm/h until it is overtaken by a flux of 0.435 cm/h, at which time a new m_- and a new m_+ are used to define the speed of the front. The process is repeated for each of the flux lines shown in Figure 6. After the shock front intersects the largest value of flux (0.435 cm/h) it intersects values less than the maximum value (e.g., values between 0.435 and 0.40). The speed of the front therefore decreases, as is shown in Figure 6. The path of the shock front can then be depicted by smoothing the stepped curve that results. The shock front begins at the snow surface at the instant at which melting first increases for the day. Actually, the shock front is modified continuously as it overtakes and interacts with values of m_+ and m_-, but for convenience we construct it in a stepwise fashion.

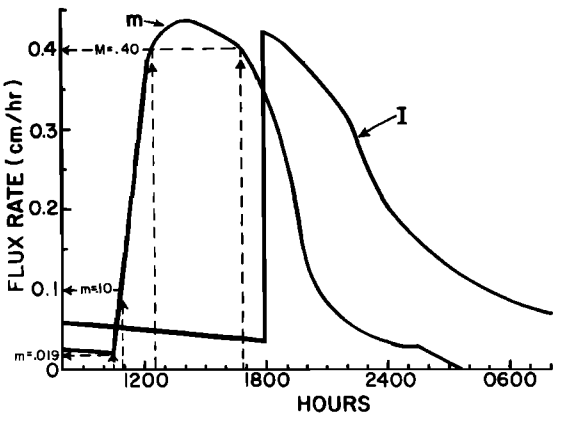

Fig. 5. Computed rates of surface melting m and output from the unsaturated zone into the saturated layer I for plot A on the tundra, May 16, 1972. Snow depth was 101 cm.

Before the shock front reaches the bottom of the snowpack ($z = 101$ cm in Figure 6), gently sloping lines from the melt of the previous day indicate the times at which these low flux rates emerge from the unsaturated portion of the pack. When the shock front reaches the bottom of the snow, there is a rapid increase of flux up to the high flux rate which arrives at that time. The maximum possible value of this flux is the peak rate of melting, but if this flux rate has already been intercepted by the shock front, the peak flux rate emerging from the unsaturated portion of the pack will be some lower rate generated at the surface after the peak of melting. In the present case the peak flux rate emerging from the unsaturated zone is 0.42 cm/h, as shown in Figures 5 and 6. After this, lines with lower slopes in Figure 6 indicate the time of arrival of fluxes on the recession limb of the hydrograph. The hydrograph of outflow from the unsaturated zone (and therefore of I, the input to the saturated layer) can be plotted, as is shown in Figure 5, by reading flux rates and times of arrival at the base of the snowpack from Figure 6.

The Saturated Zone

In order to use (6) to calculate the hydrograph from the saturated layer at the base of the slope, we must estimate the travel time through the whole saturated layer, and therefore we must estimate the permeability of the saturated layer of the snowpack. Total permeability of a porous medium is roughly proportional to the square of particle diameter [*Todd*, 1959].

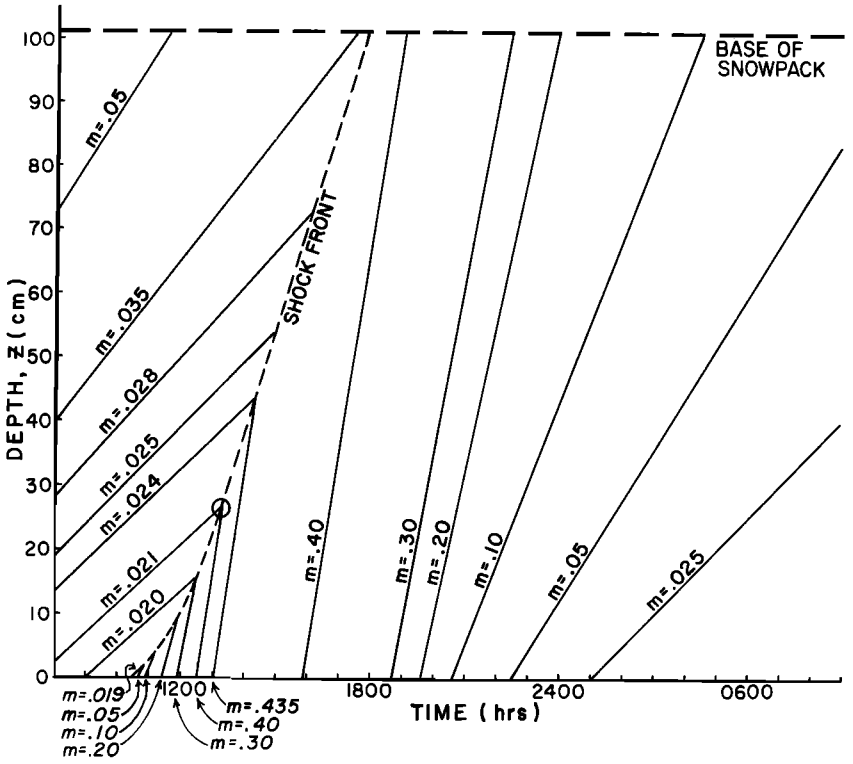

Fig. 6. Speed of values of constant flux rate originating at the surface of the snowpack ($z = 0$) at various times as indicated on Figure 5. The times at which these flux rates intersect the base of the snowpack determines the hydrograph of the input to the saturated layer.

This relationship should hold true for both the unsaturated and saturated zones, and therefore the ratio of k_s to k_u should be equal to the square of the ratio of the particle sizes. Our field measurements on the hillside plots and 5 years of regular snow pit observations in the Schefferville area indicate that the crystal sizes in the saturated layer average about 6 mm. Since this size is three times as great as that in the unsaturated zone, k_s should be equal to $9k_u$, or 54×10^{-6} cm^2. Substituting this value into (5) along with a value of 56 m for L_s (because only the lower 56 m of plot A were covered with snow on May 16) yields a value of 3.97 hours for the time of travel through the saturated layer.

The discharge arriving at the bottom of plot A at 1200 hours, for example, is the sum of all the inputs to the saturated layer over the preceding 4 hours. The result of integrating the input I in Figure 5 over this time period is shown as the computed hydrograph in Figure 7 and is there compared with the observed hydrograph for that day.

Results and Discussion

Comparison of Predicted and Observed Data

Because the graphical procedure for calculating the runoff hydrograph is time consuming, we chose a set of 20 randomly selected hydrographs for a test and analysis of the physical runoff model. The correspondence between observed and predicted hydrographs was generally good, as is shown by Figure 7 for a tundra site and Figure 8 for a more quickly responding site in the forest. The prediction of peak runoff was generally excellent, with more than half the predicted peaks lying within 10% of the observed values. For other hydrographs, however, particularly on days with low melt rates, the error ranged up to 185% of the observed value, though all other errors were less than 40%. There was a bias toward overestimation of the peak rate.

The prediction of the timing of the runoff hydrographs was less satisfactory though still remarkably good. Observed lag times between the peak rates of melting and of runoff ranged from 0.5 to 7.9 hours. Errors in the prediction of this lag varied from an underestimate of 0.2 hours to an overestimate of 2 hours. Almost all the predicted hydrographs lagged observed runoff by time periods averaging a little more than 1 hour. The timing of the rising and recession limbs of the hydrographs was similarly affected, though in a more erratic manner. In Figure 8, for example, the predicted hydrograph begins to rise 1 hour before the observed graph, even though the predicted peak is 1 hour too late.

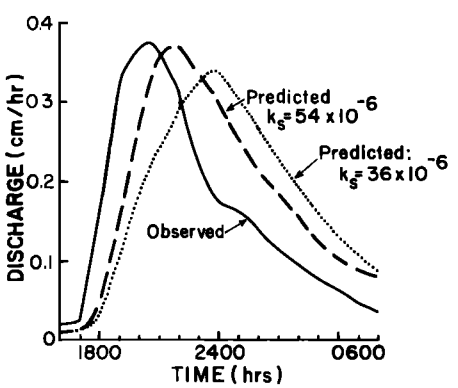

Fig. 7. Observed hydrograph and calculated outflow from the saturated layer at the base of plot A on the tundra, May 16, 1972. Two outflow hydrographs were computed by using different values for k_s with k_u held constant at 6×10^{-6} cm^2.

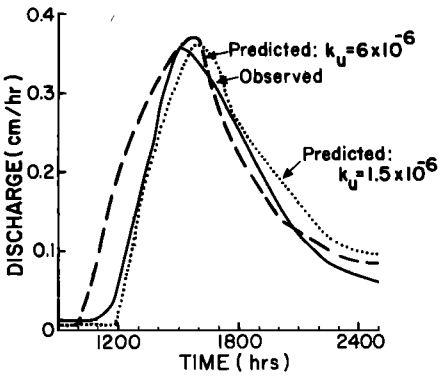

Fig. 8. Observed hydrograph and calculated outflow from the saturated layer at the base of plot E in the forest, May 9, 1973. Two outflow hydrographs were computed by using different values for k_u with k_s held constant at 54×10^{-6} cm^2.

Factors Affecting Results

We chose a value of permeability for the unsaturated zone from the literature after reviewing the characteristics of the measured snowpacks. From this value and the crystal sizes of the snowpack the permeability of the saturated zone was estimated. These estimates affect the form of the predicted hydrograph. Equations (1) and (9) indicate that the speed of both the individual fluxes and of the shock front in the unsaturated zone are proportional to the one-third power of k_u. Table 2 shows the effect upon the speed of the flux and of the shock front of varying k_u through two orders of magnitude. Higher values of k_u result in earlier arrivals of the shock front at the ground surface and faster recessions. Figure 8 shows the effect of reducing k_u to 25% of its original value while keeping k_s constant. The hydrograph began to rise 2 hours later but peaked at the same time as the original predicted hydrograph and then declined a little more slowly.

The permeability of the saturated zone affects the time of travel along the saturated path (see (3)), and therefore the period over which the input to the saturated layer must be integrated to produce the hydrograph from the base of the hillslope. As the interval of integration increases, the rates of rise and decline both decrease and the hydrograph becomes less peaked; the wave of meltwater input to the saturated layer is damped. Figure 7 illustrates the effects upon the calculated hydrograph of changing the permeability of the saturated zone. The permeability of the unsaturated layer was kept constant and the permeability of the saturated layer was reduced by $\frac{1}{3}$. This change increased the interval of integration in (6) by 50% and resulted in a hydrograph with a slower response and a lower peak, occurring two hours later than the original predicted peak. A change in permeability or an error in its estimation would have a greater effect on predicted hydrographs from a plot with a relatively deep snowpack such as A than on hydrographs from a plot with a shallow pack such as the one on E. The effect of changing permeability will also depend upon flux rate at the surface m, slope angle, and slope length.

The effects of incorrectly estimating the permeability are therefore considerable and may account for some of the timing errors in our predictions. The generally close correspondence between our predicted and observed results, however, shows that a first-chosen value of permeability from the literature, if it is based on a careful comparison of snow characteristics, can give quite accurate results.

Both $(dz/dt)_m$ and $(d\xi/dt)$ are also affected by the estimate of effective porosity, and these effects are illustrated in Table 2. Since the measurements of density on each plot showed little variation, the probable range of variation of ϕ_e is small, and its effects upon the hydrograph are small in relation to the possible effects of uncertainties about the permeability.

Snow depth is a particularly critical factor controlling the runoff response because it affects the times and rates of rise and decline of the input to the saturated layer. Therefore, for a fixed time of travel in the saturated layer, the snow depth affects the form of the discharge hydrograph from the base of the slope. Figure 9 illustrates this effect. Runoff hydrographs were computed for plot E on May 16, 1972, by using a snow depth of 56 cm (the actual depth on that day) and a hypothetical depth of 75% of this value. The shallower snowpack responds sooner and drains more rapidly. In this case the 25% difference in snow depth is not large enough to make a significant difference to the peak rate of runoff after integrating over $(t_L' - t_0')$.

In the case of plot F in Figure 9, however, the snow depth (130 cm) is large enough to have a great influence upon the form as well as the timing of the hydrograph. The hydrographs from the two plots in Figure 9 were produced from essentially the same melt pattern and the same values of ϕ, ϕ_e, k_u, and k_s. The only differences between the two plots were in the snow depth, as described above, and the time of travel through the saturated layer, which was 1.4 hours for the steeper shorter plot E and 4.2 hours for plot F. On plot E, with the shallower snowpack, the shock front reached the ground surface at 1400 hours, while on plot F it arrived at 2000 hours. When the input to the saturated layer was integrated over the longer time period, a slowly responding hydrograph with a low peak resulted, as shown in Figure 9. A further complicating effect of snow depth lies in its variation within the plot. Its effects upon the hydrograph would vary according to the pattern of snow depth, the temporal pattern of melting, and the time of travel through the saturated and unsaturated zones.

The assumption of constant slope angle was also a necessary simplification in order to make the technique manageable, and it could have led to errors with a range of magnitude and sign depending upon the profile of the hillslope, snowpack thickness, and rate of melting. The model also assumes uniformity of flow across the hillside. In one or two places on the plots, very shallow depressions in the ground surface must have

TABLE 2. Effects of Variation of Parameters Upon the Predictions of the Percolation in the Unsaturated Zone

Variable Parameter	Chosen Constant Values	$(dz/dt)_m$, cm/h	$d\xi/dt$, cm/h
$k_u = 6 \times 10^{-7}$ cm^2	$m = 0.325$ cm/h; $\phi_e = 0.652$	10.8	
$k_u = 6 \times 10^{-6}$ cm^2		23.0	
$k_u = 6 \times 10^{-5}$ cm^2		50.0	
$k_u = 6 \times 10^{-7}$ cm^2	$u_- = 0.025$ cm/h; $u_+ = 0.325$ cm/h; $\phi_e = 0.652$		7.2
$k_u = 6 \times 10^{-6}$ cm^2			15.4
$k_u = 6 \times 10^{-5}$ cm^2			33.4
$\phi_e = 0.552$	$m = 0.325$; $k_u = 6 \times 10^{-6}$ cm^2	26.5	
$\phi_e = 0.652$		23.0	
$\phi_e = 0.752$		19.5	

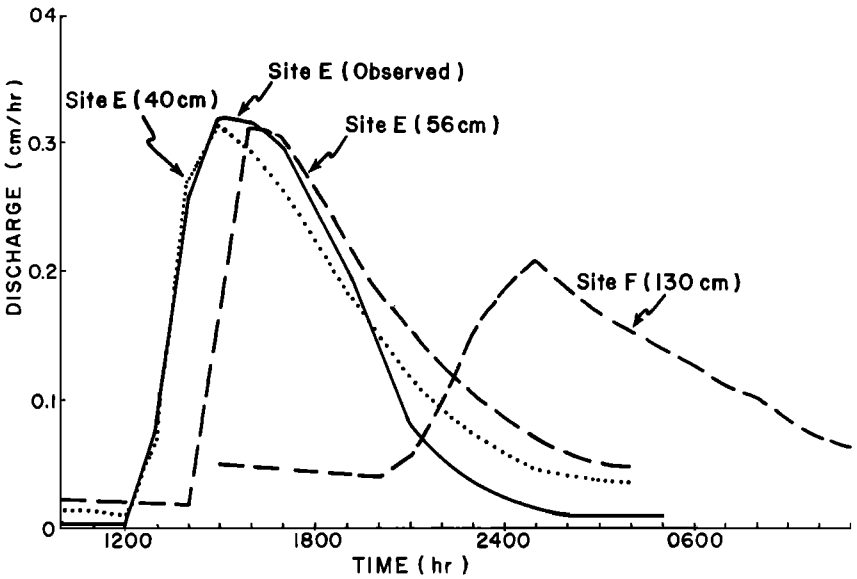

Fig. 9. Observed hydrograph and hillslope discharge from plot E computed by using the actual snow depth of 56 cm and a hypothetical snow depth of 42 cm. The computed outflow hydrograph from plot F is also shown. Because of instrument failure the hydrograph from plot F was not measured, but the predicted and observed hydrographs from this plot agreed closely on other days.

concentrated the flow, but the slopes were generally smooth enough for the idealization to be valid. At several times during the melt we dug into the snowpack to measure the thickness of the saturated layer. It was not possible to make many such measurements without destroying the snowpack, but the few results that we obtained were consistent with the model. The thickness of the saturated layer increased downslope at any one time from zero at the top of the slope to as much as 2.7 cm, 40 m from the top of plot E on a day of moderately high melt rate. At any one point on the slope the saturated layer increased rapidly from a small unmeasurable value in the late morning to a maximum in the middle of the day, and then decreased slowly. The amplitude of the variation increased downslope, as the model predicts.

Finally, errors in the prediction of the runoff hydrographs can result from errors in the hourly computation of melt.

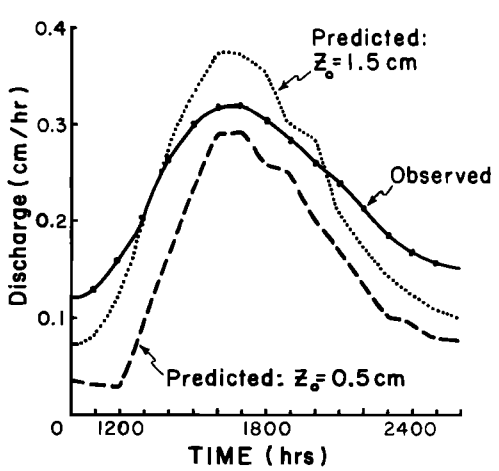

Fig. 10. Effect on the predicted hydrograph of changing the roughness length (z_0) of the snow surface on a day with high turbulent heat flow to the snowpack of plot G in the forest on May 11, 1973. Daily total melt calculated with z_0 = 0.5 cm was 3.11 cm; with z_0 = 1.5 cm, the calculated melt was 4.18 cm; the observed melt was 4.95 cm.

Errors in the predicted hydrographs were greatest on the days when the energy balance model produced inaccurate results [see *Price and Dunne*, 1976]. On May 11, 1973, for example, the total daily melt on plot G was badly underestimated. The predicted daily total was 3.11 cm, while the measured melt was 4.95 cm. The computed hourly fluxes m must also have been too low, leading to the underestimation of the rate of travel of all the fluxes and of the shock front and to the computation of a hydrograph that rises later than the observed hydrograph. Some hydrographs from days when fluxes were underestimated also peaked 1–2 hours after the observed peak discharge.

In our earlier paper on the energy balance we suggested that the change in roughness length of the snow surface was an important factor causing the underestimation of melt rates. We made an estimate of the roughness length late in the season on the basis of the height of protruding vegetation and recomputed melt rates with the new value. When we calculated runoff hydrographs using the new melts rates, both $(dz/dt)_m$ and $(d\xi/dt)$ increased, and the hydrographs became more peaked and occurred earlier. In the example shown in Figure 10, the predicted hydrograph agrees closely with the field observations except that the peak is overestimated. For some other hydrographs the change in the energy balance computation gave much better agreement between observed and calculated peaks. It is clear then that for accurate prediction of snowmelt runoff hydrographs from individual hillsides the energy balance of the snowpack needs to be defined with great precision.

On days when the snowmelt prediction was accurate, however, the model gave remarkably good results. Figure 11 shows a comparison between predicted and observed values of peak runoff and lag times for the random sample of 20 hydrographs chosen for prediction. The work demonstrates the feasibility of applying models based on sound physical principles to the understanding and prediction of snowmelt runoff from hillsides under a range of cover, topography, and snowpack conditions. At present, limitations of data acquisition may limit the applicability of this model to hydrologic forecasting, but as

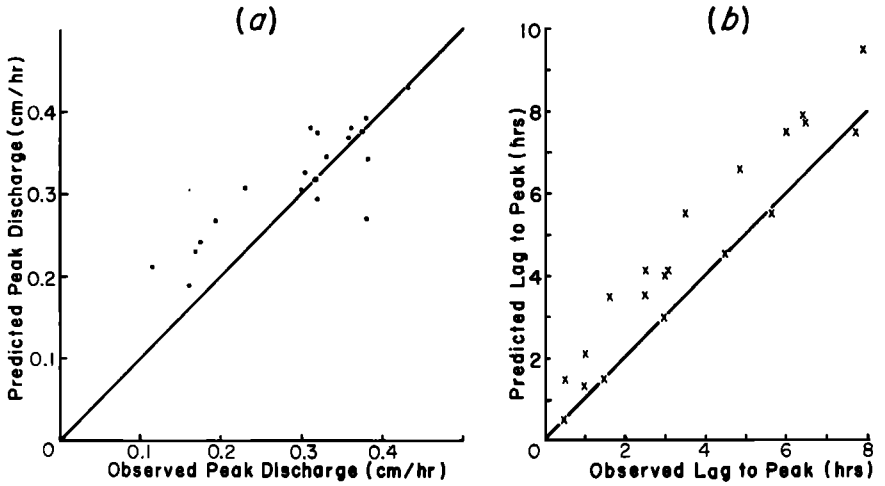

Fig. 11. Comparison of predicted and observed values of (*a*) peak discharge and (*b*) lag to peak (defined as the time difference between the peak of surface melting and the peak of runoff).

this study shows, the model can be used as a basis for deciding which measurements would be most beneficial.

NOTATION

C_s wave speed in the saturated layer, centimeters per hour.
$(dz/dt)_m$ rate of vertical travel of a constant flux m, centimeters per hour.
$(d\xi/dt)$ rate of propagation of the shock front, centimeters per hour.
g acceleration due to gravity, centimeters per hour per hour.
h thickness of the saturated layer, centimeters.
I rate of input to the saturated layer, cubic centimeters per square centimeter per hour.
$k(S)$ permeability of the unsaturated zone at some fixed value of S, square centimeters.
k_s intrinsic permeability of the saturated zone, square centimeters.
k_u intrinsic permeability of the unsaturated zone, square centimeters.
L_s length of the hillside plot, centimeters.
m rate of melting and of flux at the snowpack surface, cubic centimeters per square centimeter per hour.
n an exponent.
q discharge from the base of the hillside, cubic centimeters per centimeter width of hillside per hour.
Q discharge from the base of the hillside, centimeters per hour.
S degree of saturation of the snowpack.
S_i irreducible saturation of the snowpack.
t, t' time, hours.
t_0' initial time, hours.
t_L' time required for a parcel of water to traverse the entire length of the hillside in the saturated layer, hours.
x, x' distance along the hillslope, centimeters.
z depth in the snowpack, centimeters.
β inclination of the hillslope, degrees.
μ viscosity of water, grams per hour per centimeter.
ρ density of water, grams per cubic centimeter.
ρ_i density of ice, grams per cubic centimeter.
ϕ total porosity of the saturated zone of the snowpack.
ϕ_e effective porosity of the unsaturated zone of the snowpack.

Acknowledgments. This study was carried out while two of us (T. D. and A. G. P.) worked at McGill University. It was supported by grants from the National Research Council of Canada, the Canadian Department of Environment, and the Iron Ore Company of Canada. (S.C.C. was supported by DA project 4A161102B52E/02 at CRREL.) We are grateful to F. H. Nicholson of the McGill Subarctic Research Laboratory and to J. E. Fitzgibbon, M. N. Nicholson, D. E. Petzold, and R. G. Wilson of the geography department at McGill University for their assistance and company in some trying conditions.

REFERENCES

Anderson, E. A., Development and testing of snowpack energy balance equations, *Water Resour. Res.*, *4*(1), 19–37, 1968.
Colbeck, S. C., One-dimensional theory of water flow through snow, *Res. Rep. 296*, 17 pp., U.S. Army Cold Reg. Res. and Eng. Lab., Hanover, N. H., 1971.
Colbeck, S. C., A theory of water percolation in snow, *J. Glaciol.*, *11*(3), 369–385, 1972.
Colbeck, S. C., On predicting water runoff from a snow cover, in *Advanced Concepts and Techniques in the Study of Snow and Ice Resources*, edited by H. S. Santeford and J. L. Smith, pp. 55–66, 1974*a*.
Colbeck, S. C., Water flow through snow overlying an impermeable boundary, *Water Resour. Res.*, *10*(1), 119–123, 1974*b*.
Colbeck, S. C., and G. Davidson, Water percolation through homogeneous snow, in *The Role of Ice and Snow in Hydrology, IASH Publication 107*, vol. 1, pp. 242–257, International Association of Scientific Hydrology, Geneva, 1973.
Dunne, T., and R. D. Black, Runoff processes during snowmelt, *Water Resour. Res.*, *7*(5), 1160–1172, 1971.
Gerdel, R. W., Dynamics of liquid water in deep snowpacks, *Eos Trans. AGU*, *26*, 83–90, 1945.
Post, F. A., and F. R. Dreibelbis, Some influences of frost penetration and microclimate on the water relationships of woodland, pasture and cultivated soils, *Soil Sci. Soc. Amer. Proc.*, *7*, 95–104, 1942.
Price, A. G., Snowmelt runoff processes in a subarctic area, Ph.D. dissertation, 185 pp., McGill Univ., Montreal, Quebec, 1975.
Price, A. G., and T. Dunne, Energy balance computations of snowmelt runoff in a subarctic area, *Water Resour. Res.*, *12*, this issue, 1976.
Shimizu, H., Air permeability of deposited snow, *Low Temp. Sci. Ser. A*, *22*, 1–32, 1970.
Todd, D. K., *Groundwater Hydrology*, 336 pp., John Wiley, New York, 1959.

(Received November 25, 1975;
accepted February 17, 1976.)